Automatic Screening and Staging of Multi-Stage Diabetic Retinopathy using Deep Learning techniques

Hardik Srivastava[1] and Dr. T. Rajalakshmi[2]
Department of Computer Science Engineering[1]
Department of Electronics and Communication Engineering[2]
SRM Institute of Science and Technology
hs9644@srmist.edu.in [1] and rajalakt@srmist.edu.in [2]

Abstract— **Diabetic retinopathy is a consequence of diabetes that is caused by damage to the blood vessels of the light-sensitive tissue called the retina. It is the main cause of visual impairment and blindness among working-age individuals, as well as the most common cause of vision loss among diabetics. Recent advancements in the usage of automated systems for diabetic retinopathy diagnostics have presented new problems to the industry, including the hunt for a less resource-intensive architecture, such as the creation of a low-cost embedded software. In this paper we propose a novel noise compatible and balanced system for automatic screening and diagnosis of Diabetic Retinopathy using Deep Convolutional Neural Networks along with a comparative study between the different state-of-the-art algorithms employed for automatic DR screening. A total of 35,127 eye fundus-colored numerical images were obtained from the 4th Asia Pacific Tele-Ophthalmology Society (APTOS) Symposium and Kaggle, in collaboration with the California Healthcare Foundation and EyePacs, which is a free platform for retinopathy screening. The images were graded as No Apparent DR (25,810 images), Mild Non-Proliferative DR (NPDR) (2443 images), Moderate NPDR (5292 images), Severe NPDR (873 images), and Proliferative DR (PDR) (708 images) using existing datasets. This approach can automatically detect diabetic retinopathy with an accuracy of 88.6% and could aid in making a referral recommendation for further evaluation and treatment with high reliability.**

Index Terms—**Diabetic Retinopathy, Deep CNNs, Fundus images, Retinal Image Processing, Medical Imaging.**

I. INTRODUCTION

Diabetes mellitus (DM) is one of the large-scale causes of death worldwide [3, 4], and the prevalence of DM continues to increase. Eighty to eighty-five percent of the patients suffering with diabetes for more than 10 years have a high risk of eye issues which affects the retina of the eyes. Diabetic Retinopathy (DR) is an eye disorder that leads to severe consequences and people may tend to lose vision as a result of this condition when it reaches its extreme stages. The medical tests for DR encompass several procedures, time, poor accuracy and money to detect the presence of the proliferative stage of DR. Hence, automated detection of DR with multiple stages is considered an important technique for diagnosis.
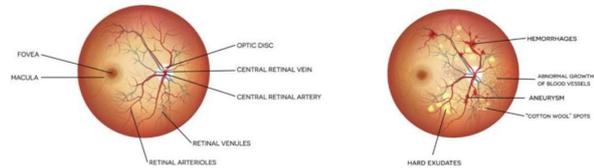

Figure 1: Comparison between a normal eye and a DR affected eye

Deep learning approaches have been successful and promising for medical image analysis [5]. Deep learning is a branch of machine learning that aims at extracting and learning various higher-level features from the raw input, here images. With each level learning to transform its input data into a slightly more abstract and composite representation, this allows for successful classification, detection and staging of the disease.

The objective of this work is to develop a noise-compatible and balanced system for the detection of diabetic retinopathy. We have employed deep learning methodologies for detection and interpretation of microscopic retina images based on the various grades used to scale the severity of diabetic retinopathy, namely No DR, Mild, Moderate, Severe and Proliferative DR. We have made use of three state-of-the-art architectures, EfficientNet, ResNet, and the VGGNet, in this work and made a comparative analysis amongst the results obtained by them after training and validation. Fig. 2 shows the proposed methodology for our work. Diabetic Retinopathy Detection can be viewed from several perspectives: as a classification problem, as a regression problem, and as an ordinal regression problem (Ananth and Kleinbaum, 1997). This is because different stages of the disease come sequentially. The proposed model provides a promising solution that will enable ophthalmologists better assess the disease and track its progression without the need for any subjective assessment. The remnant of this proposed paper is organized as follows. Section II provides a detailed explanation of the proposed models used for the computer-aided diagnosis and classification of DR. The proposed network architecture is explained in Section III and the statistical

evaluation, and experimental results are then discussed in Section IV. Finally, the conclusion and summary are presented in the last section.
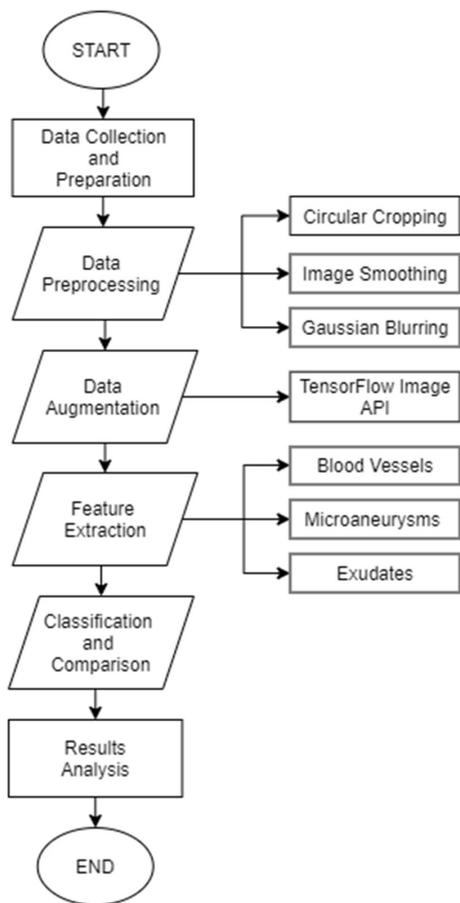

Figure 2: Proposed Methodology

II. EXPERIMENTAL METHODOLOGY

The process flow of Methods and Methodology adopted to carry out the present work is shown in Fig. 2. Subsequent subsections describe the pre-processing of retinal fundus images for classifying and finding the accuracy of the proposed models which help in the precise detection of diabetic retinopathy.

A. Dataset

The retina images utilized in this work for computer-assisted diagnosis of diabetic retinopathy are obtained from the 2019 APTOS Symposium. The dataset contains 35,127 high-resolution microscopic human retina images under a variety of imaging conditions. Fig. 3 show the class distribution of our dataset. These retina images were acquired by 3 ophthalmologic departments using a color video 3CCD camera mounted on a Topcon TRC NW6 non-mydriatic retinograph with a 45-degree field of view. Images were captured using 8 bits per color plane

at 1440*960, 2240*1488, or 2304*1536 pixels. For each subject, two images were obtained for the left and right eyes respectively. The labels were provided by clinicians who marked the presence of diabetic retinopathy with a corresponding scale that reflects its severity. Table 1 shows the class indices along with their grades and associated lesions. The sample images are shown in Fig. 4.
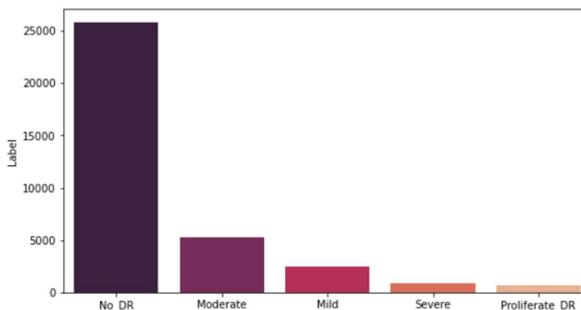

Figure 3: Class distribution of Fundus Images

Class Index	No. of images	Grade	Lesions
0	25810	No DR	Absence of lesions
1	2443	Mild	MA only
2	5296	Moderate	More than MA but less than severe DR
3	873	Severe	Any of the following: • More than 20 intraretinal HM in each of 4 quadrants • Definite venous beading in 2+quadrants • Prominent intraretinal microvascular abnormalities in 1+ quadrant • No signs of proliferative DR
4	708	Proliferate DR	One or more of the following: vitreous/pre-retinal HM, neovascularization

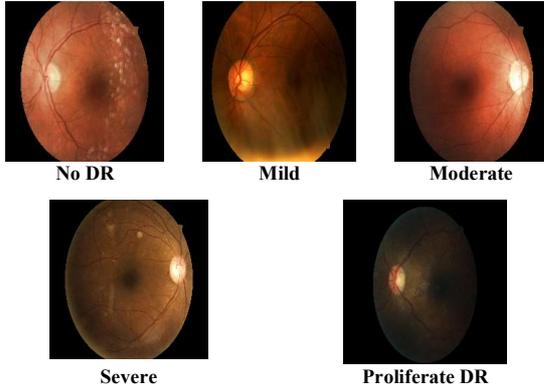*Table 1: Levels of Diabetic Retinopathy along with their associated lesions*

No DR **Mild** **Moderate**

Severe **Proliferate DR**

Figure 4: Stages 0-4 of Diabetic Retinopathy with their labels

B. Data Pre-processing

Model training and validation are performed on the pre-processed versions of the original images. The pre-processing methods comprised of image cropping and smoothing followed by resizing. Image cropping is necessary to cut out the black region around the retina image as it may affect training by adding noise. Pre-processing needs to be performed to get all retina images in a standard format. Additionally, as the type of data that the model will come across while testing isn't predictable, we decided to show as much data variance as possible to the models. Following things are carried out while pre-processing:

• *Resizing images*: The original images are of various sizes with some images having side lengths of 4000 pixels. To make the training and feature extraction efficient, all images are resized to 224 x 224.

• *Image cropping*: The black background of the fundus images is discarded as it doesn't provide any valuable information to the model.
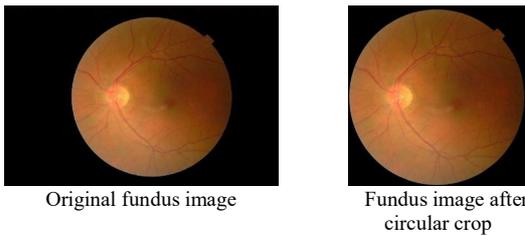

Original fundus image Fundus image after circular crop

Figure 5: Removing noise with circular crop followed by smoothening of sharp corners

• Smoothing corners: After removing the black background, the corners of the image are smoothened to remove any sharp edges.
• Gaussian Blur: A Gaussian filter is finally applied to all the images to remove any noise. Fig. 6 shows a Gaussian Filtered retina image.

Figure 6: Fundus image after Gaussian filtering

C. Gaussian Smoothing

The Gaussian smoothing operator is a 2-D convolution operator frequently employed in computer vision tasks. It is used to blur images and remove any prevalent noise. Fig. 7 shows a Gaussian distribution in 1-D with mean 0 and $\sigma = 1$.

The Gaussian distribution in 1-D has the following form:

$$f(x) = \frac{1}{\sigma\sqrt{2\pi}} e^{-\frac{1}{2}\frac{(x-\mu)^2}{\sigma^2}} \tag{1}$$
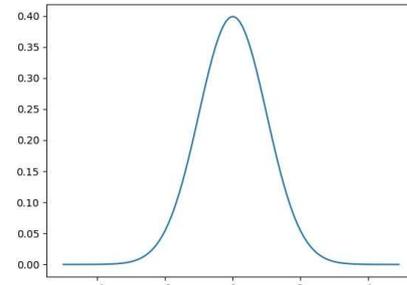

Figure 7: Gaussian distribution in 1-D

In 2-D, the Gaussian distribution takes the following form for mean (0,0) and $\sigma = 1$:

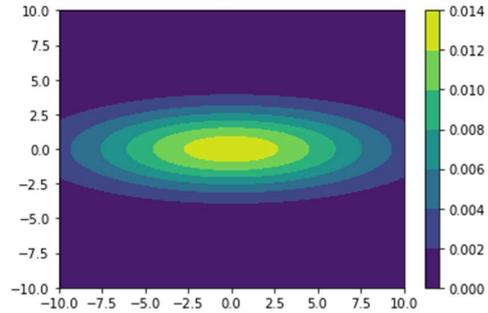$$f(x) = \frac{1}{2\pi\sigma^2} e^{-\frac{x^2+y^2}{2\sigma^2}} \tag{2}$$

Figure 8: Gaussian distribution in 2-D

Gaussian smoothing works in a similar way as the mean filter [6]. The standard deviation of the Gaussian σ determines the degree of smoothing. The Gaussian function returns a `weighted average' of each pixel's neighborhood, with the average weighted more towards the center pixel's value. This is in contrast to the uniformly weighted average of the mean filter. As a result, a Gaussian smoothens an image more gently and preserves the edges better than a similarly sized mean filter.

D. Data Augmentation

Image transformation techniques like translation, stretching, rotation, flipping, and color augmentation are used for data augmentation. TensorFlow 2.0 provides random transformations to augment images like horizontal flip, vertical flip, random rotation, random shift, random scale, a shift of RGB values, random brightness and contrast, additive Gaussian noise, blur, sharpening, embossing, random gamma, cut-out, etc.

• Rotations: The following affine transformation A, where θ is between 10 and 175 degrees, is applied. The images were randomly rotated in the range of ± 30°.

$$A = \begin{pmatrix} \cos\theta & -\sin\theta \\ \sin\theta & \cos\theta \end{pmatrix} \quad (3)$$

• Shears: Finally, each image I is sheared by a range of 0.15, represented by the following affine transformation A. s defines the amount that I is sheared, and it is in the range of [0.1, 0.35].

$$A = \begin{pmatrix} 1 & s \\ 0 & 1 \end{pmatrix} \quad (4)$$

• Random Zoom: The images were randomly zoomed by a random amount within the range [-10%, 10%], with bilinear interpolation and reflective fill mode, reducing edge artifacts.

III. Network Architecture

Our work aims to classify each fundus image accurately. We have utilized EfficientNet [7], ResNet [8] and VGGNet [9] for a comparative analysis based on the model performances on the retina images. The outputs of the convolutional and early fully connected layers are processed using the Rectified Linear Unit (ReLU) [10] activation function defined as follows:

$$a_i = \begin{cases} b_i, & b_i > 0 \\ 0, & b_i < 0 \end{cases} \quad (5)$$

where b_i is the input to ReLU and a_i is the corresponding activation. However, in the end of the network, the softmax activation function is deployed to predict a probability distribution of each of the FC layer outputs as follows:

$$a_i = \frac{e^{-c_i}}{\sum_{j=0}^{L} e^{-c_i}} \quad (6)$$

where c_i is the ith output of the FC layer, L is the number of classes and a_i is the activation. We have used a sequential modeling approach for adding and customizing the different layers of the neural network with a categorical cross-entropy loss function which is minimized using the Stochastic Gradient Descent (SGD) in order to update the model parameters.

$$e = -\sum_{j=0}^{L} \hat{a}_j \, log(a_j) \quad (7)$$

where e is the cross-entropy loss and $\hat{a}_j$ is the expected desired probability.

1. EfficientNet: EfficientNet is a convolutional neural network architecture and scaling method that uniformly scales all dimensions of depth/width/resolution using a compound coefficient. Generally, we can define a convolutional layer as a tensor function, namely $Y_i = F_i(X_i)$, where Y_i is the output tensor, F_i is the tensor operator, and X_i is the input tensor. The shape of the input tensor is (H_i, W_i, C_i), where H_i and W_i are the spatial dimensions and C_i is a color dimension. One should define the model of convolutional networks as a sequence of embedded functions (Mingxing Tan, Quoc V. Le, 2019), where F_i^L is a layer repeated L times at stage i.

$$N = \odot \, F_i^L \left(X_{(H_i, W_i, C_i)} \right)_{i=1..n} \quad (8)$$

Depth: $d = \alpha^\Phi$ (9)
Width: $w = \beta^\Phi$ (10)
Resolution: $r = \gamma^\Phi$ (11)
Constraints: $\beta^2 . \gamma^2 \approx 2; \; \alpha \geq 1; \; \beta \geq 1; \; \gamma \geq 1$
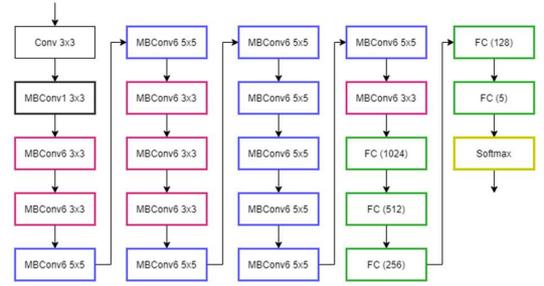

Figure 9:Architecture of the proposed EfficientNetB0 model

We utilized the EfficientNetB0 network and instantiated it with 'imagenet' weights. The last layer of the network is excluded to add 4 Dense layers to extract more deep features in the eye retina and finally an output Dense layer with a softmax activation function to predict a multinomial probability distribution. Table 2 shows the model summary.

Layer (type)	Output Shape	Param #
efficientnet-b0 (Functional)	(None, 7, 7, 1280)	4049564
flatten_1 (Flatten)	(None, 62720)	0
dense_1 (Dense)	(None, 1024)	64226304
dense_2 (Dense)	(None, 512)	524800
dense_3 (Dense)	(None, 256)	131328
dense_4 (Dense)	(None, 128)	32896
dense_5 (Dense)	(None, 5)	645

Table 2: Proposed EfficientNetB0 model summary

2. ResNet: Residual Networks are known to solve the problem of vanishing gradients by utilizing skip connections to jump over some layers. The network then tends to gradually restore the skipped layers as it learns the feature space. Residual Networks speed up the training of very deep neural networks and increase the

model's accuracy on large training data:

$$H(x) = F(x) + x \quad (1) \qquad (12)$$

Here, x is the input of the building block and F(x) represents the output of the layer within the building block of the residual network.
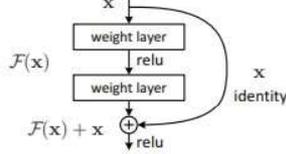

Figure 10: The basic building block of a Residual Network

We utilized the ResNet50 model which has 48 convolutional layers along with 1 MaxPool and 1 AveragePool layer. To avoid overfitting, we used Batch Normalization and dropout of 0.5 in-between the Dense layers. The last layer of the network is a Dense layer with 5 neurons for output. Table 4 shows the model summary.

Layer (type)	Output Shape	Param #
resnet50 (Model)	(None, 1, 1, 2048)	23587712
flatten (Flatten)	(None, 2048)	0
dense_1 (Dense)	(None, 128)	262272
dropout_1 (Dropout)	(None, 128)	0
batch_normalization_1 (Batch Normalization)	(None, 128)	512
dense_2 (Dense)	(None, 64)	8256
dropout_2 (Dropout)	(None, 64)	0
batch_normalization_2 (Batch Normalization)	(None, 64)	256
dense_3 (Dense)	(None, 5)	325

Table 3: ResNet50 model summary used in this work

3. VGGNet: VGG19 consists of 19 layers where there are 16 convolution layers, 3 Fully connected layer, 5 MaxPool layers and 1 Softmax layer. VGG19 is convenient because of its simplicity as 3*3 convolutional layers are mounted on the top to increase with the depth level. The convolutional layers in VGG-19 are used for feature extraction and the max pooling layers, which act as handlers for VGG-19, associated with some of the convolutional layers are responsible for feature dimensionality reduction. FC layers are used to prepare the feature vector. Table 4 shows the model summary.

Layer (type)	Output Shape	Param #
vgg19 (Model)	(None, 7, 7, 512)	2359808
global_average_pooling_2d (Global Average Pooling 2D)	(None, 512)	0
dense (Dense)	(None, 128)	65664
dense_1 (Dense)	(None, 128)	16512
dense_2 (Dense)	(None, 5)	645

Table 4: VGG-19 model summary used in this work

A. Training Specifications

The network architecture has already been discussed; this section focuses on other technical details. The network is designed and trained with TensorFlow 2.4.1 using TPUs (Tensor Processing Units) on Google Colaboratory. Each of the architectures is trained for 100 epochs. The optimizer used is Adam to optimize the weights during training with a learning rate of 0.001.

IV. STATISTICAL EVALUATIONS

For the purpose of evaluating the performance of the proposed deep transfer learning approach for identifying DR, overall classification accuracy, classification sensitivity (Sensitivity), and specificity (Specificity) were calculated, and the performance of the best model was further compared to results obtained by retinal specialists. The statistical analysis was performed using statistical software (Python ver. 3.8.3) implementing NumPy, SciPy, statsmodels, and Scikit-learn modules. Accuracy is defined as the ratio of the number of correctly labelled images to the overall number of test images. Sensitivity is calculated by dividing the number of true positive TP by the sum of total number of true positives and false negatives (TP + FN). Specificity is defined as a ratio of the number of true negatives TN to the sum of the number of true negatives and false positives (TN + FP), describing the ratio of no referral cases correctly categorized by the algorithm.

$$Accuracy = \frac{TP + TN}{TP + FP + TN + FN} \qquad (13)$$

$$Sensitivity = \frac{TP}{TP + FN} \qquad (14)$$

$$Specificity = \frac{TN}{TN + FP} \qquad (15)$$

Based on the True Positives (TP), True Negatives (TN), False Positives (FP), and False Negatives (FN) results, the accuracy is predicted. In this proposed work, normal samples were taken as positive case, and DR disorder patients were considered as the negative case. Normal subjects correctly classified as healthy termed as TP, DR patients correctly classified as DR case considered as TN, DR patients misclassified as healthy treated as FP, and normal subjects incorrectly classified as patients termed as FN.

The measure of inter-rater reliability for categorical items or two individual items is known as Cohen's kappa coefficient (κ). The value of Cohen's kappa is calculated as:

$$\kappa = \frac{p_0 - p_e}{1 - p_e} \qquad (17)$$

A. Results and Discussions

In this section, we tested EfficienNetB0, ResNet50 and VGG19 deep learning models to classify fundus images. The results confirm that utilizing the existing deep learning architectures using Transfer Learning has the potential to substantially improve DR detection performance. The results of EfficienNetB0, ResNet50 and VGG19 models are provided with a performance comparison in Table 6 and the conclusions are examined in detail.

For EfficientNet, we obtained an accuracy of 88.6%. Initially, EfficientNet was trained for 60 epochs only. Since 60 epochs took around 9 hours to train on a GPU with considerably high loss, this was estimated to be too short a time to be able to extract any substantial deep features to obtain some useful information, therefore the model was re-trained for 100 epochs with an early stopping function to monitor the generalization error and prevent overfitting in the worst case. EfficientNetB0 provided a Cohen's kappa value of 0.8473. The sensitivity came out to be 88.9% and the specificity was around 83.1%. Figs. 11, 12, 13 and 14 represent the confusion matrix calculated for EfficientNetB0 and the accuracy and loss curves for all the three architectures we experimented on in this work.

Figure 11: Confusion matrix for our proposed EfficientNetB0 model when tested on the validation dataset
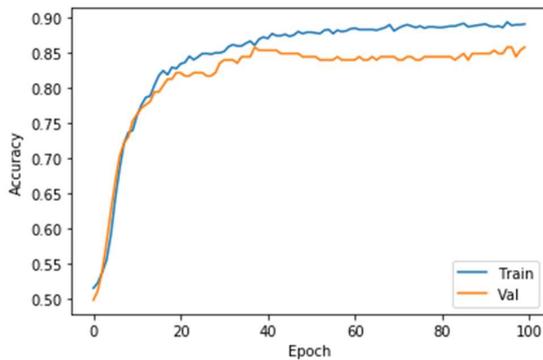

Figure 12: Curve showing the accuracy values our proposed model achieved during training and validation

For ResNet50, we achieved a validation accuracy of around 72%. The problem with most of the residual networks is that when its depth increases, the problem of vanishing gradient also increases. It directly affects the weights as they never update their values and no learning is achieved saturating the accuracy and the network has trouble reaching convergence. The Cohen's kappa value for Resnet50 was 0.58415.
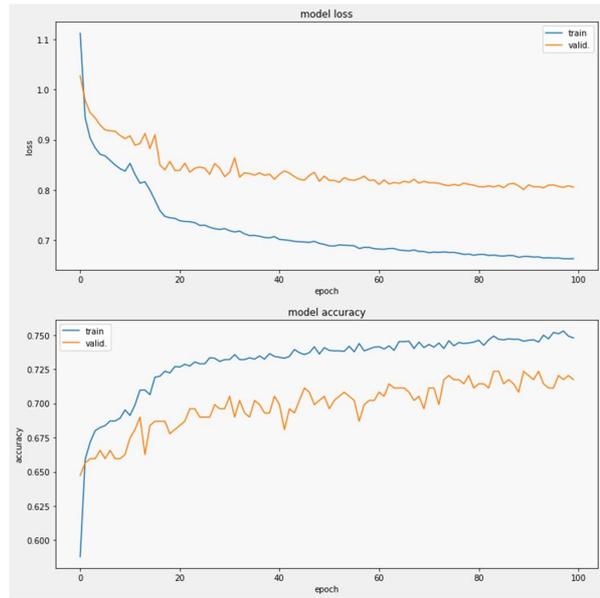

Figure 13: Accuracy and Loss curves for ResNet50

For VGG19, the validation accuracy was around 74%. The Cohen's kappa value obtained for VGG19 model was 0.6147.
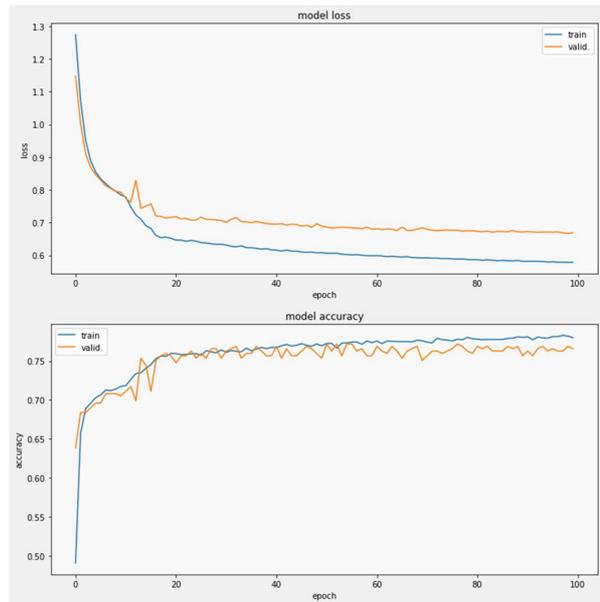

Figure 14: Accuracy and Loss curves for VGG-19

CLASSIFIER	DATA SET	ACC.	κ VALUE	DR CLASSES
EfficientNetB0	APTOS 2019	89%	0.8473	No DR, Mild, Moderate, Severe and Proliferative DR
VGG-19	APTOS 2019	74%	0.6147	No DR, Mild, Moderate, Severe and Proliferative DR
ResNet50	APTOS 2019	72%	0.5842	No DR, Mild, Moderate, Severe and Proliferative DR

Table 5: Results of experiments and metrics tracked

Going by the results and the κ value, EfficientNet provided much better results as compared to ResNet50 and VGG-19.

V. CONCLUSION

Diabetic Retinopathy (DR) is a complication of long-standing, unchecked diabetes, and one of the leading causes of blindness in the world. In practice, doctors can recognize DR by looking for lesions related with the disease's vascular anomalies. While this strategy is effective, it necessitates a lot of resources. The numerical experiments of this work were conducted on the Asia Pacific Tele-Ophthalmology Society (APTOS) 2019 dataset. A deep convolutional neural network that uses compound scaling for better complexity and performance was introduced that could extract deep features from the pre-processed fundus images at even lower complexities and could accurately classify them and stage DR into normal retinas, mild NPDR, moderate NPDR, severe NPDR and proliferative DR (PDR). This method will help ophthalmologists and health practitioners in direct detection of retinopathy and faster interpretation of the severity of the disorder, such that it can be used as a screening and decision support tool with higher accuracy and reliability for faster diagnosis. In the future, we aim to extend our proposed architecture to work on the real-world unfiltered data in real-time for clinical applications. We also aim to train images of various modalities using the suggested CNN model with our modifications in the future to further increase the accuracy of the proposed technique. We will also use capsule networks to classify fundus images, which were recently developed by Geoffrey Hinton [11].

REFERENCES

[1] APTOS 2019 Blindness Detection

[2] EyePacs — free platform for retinopathy screening.

[3] World Health Organization, 2016. Global report on diabetes. Address: http://www.who.int

[4] Saaddine, J.B., Honeycutt, A.A., Narayan, K.V., Zhang, X., Klein, R. and Boyle, J.P., 2008. Projection of diabetic retinopathy and other major eye diseases among people with diabetes mellitus: United States, 2005- 2050. Archives of ophthalmology, 126(12), pp.1740-1747.

[5] Yau, J.W., Rogers, S.L., Kawasaki, R., Lamoureux, E.L., Kowalski, J.W., Bek, T., Chen, S.J., Dekker, J.M., Fletcher, A., Grauslund, J. and Haffner, S., 2012. Global prevalence and major risk factors of diabetic retinopathy. Diabetes care, 35(3), pp.556-564.

[6] G. George, R. M. Oommen, S. Shelly, S. S. Philipose and A. M. Varghese, "A Survey on Various Median Filtering Techniques For Removal of Impulse Noise From Digital Image," 2018 Conference on Emerging Devices and Smart Systems (ICEDSS), 2018, pp. 235-238, doi: 10.1109/ICEDSS.2018.8544273.

[7] Mingxing Tan and Quoc V. Le. EfficientNet: Rethinking Model Scaling for Convolutional Neural Networks. ICML 2019. Arxiv link: https://arxiv.org/abs/1905.11946.

[8] K. He, X. Zhang, S. Ren and J. Sun, "Deep Residual Learning for Image Recognition," 2016 IEEE Conference on Computer Vision and Pattern Recognition (CVPR), 2016, pp. 770-778, doi: 10.1109/CVPR.2016.90.

[9] S. Liu and W. Deng, "Very deep convolutional neural network based image classification using small training sample size," 2015 3rd IAPR Asian Conference on Pattern Recognition (ACPR), 2015, pp. 730-734, doi: 10.1109/ACPR.2015.7486599.

[10] K. Hara, D. Saito and H. Shouno, "Analysis of function of rectified linear unit used in deep learning," 2015 International Joint Conference on Neural Networks (IJCNN), 2015, pp. 1-8, doi: 10.1109/IJCNN.2015.7280578.

[11] E. Dash, J. Mercy Faustina and B. Sivaselvan, "Representative Primary Capsule in Capsule Network Architecture for Fast Convergence," 2020 IEEE 4th Conference on Information & Communication Technology (CICT), 2020, pp. 1-6, doi: 10.1109/CICT51604.2020.9312064.

[12] Duh, E.J., Sun, J.K. and Stitt, A.W., 2017. Diabetic retinopathy: current understanding, mechanisms, and treatment strategies. JCI insight, 2(14).

[13] Wilkinson, C.P., Ferris III, F.L., Klein, R.E., Lee, P.P., Agardh, C.D., Davis, M., Dills, D., Kampik, A., Pararajasegaram, R., Verdaguer, J.T. and Group, G.D.R.P., 2003. Proposed international clinical diabetic retinopathy and diabetic macular edema disease severity scales. Ophthalmology, 110(9), pp.1677-1682.

[14] Salz, D.A. and Witkin, A.J., 2015. Imaging in diabetic retinopathy. Middle East African journal of ophthalmology, 22(2), p.145.

[15] Fong, D.S., Aiello, L., Gardner, T.W., King, G.L., Blankenship, G., Cavallerano, J.D., Ferris, F.L. and Klein, R., 2004. Retinopathy in diabetes. Diabetes care, 27(suppl 1), pp.s84-s87.

[16] Vitale, S., Maguire, M.G., Murphy, R.P., Hiner, C., Rourke, L., Sackett, C. and Patz, A., 1997. Interval between onset of mild nonproliferative and proliferative retinopathy in type I diabetes. Archives of Ophthalmology, 115(2), pp.194-198.

[17] Deng, J., Dong, W., Socher, R., Li, L.J., Li, K. and Fei-Fei, L., 2009, June. Imagenet: A large-scale hierarchical image database. In 2009 IEEE conference on computer vision and pattern recognition (pp. 248- 255).

[18] J. Liang, W. Pei, and F. Lu, "Cpgan: Content-parsing generative adversarial networks for text-to-image synthesis," in European Conference on Computer Vision. Springer, 2020, pp. 491–508.

[19] S. Fiorini, L. Ballerini, E. Trucco, and A. Ruggeri, "Automatic generation of synthetic retinal fundus images." in Eurographics Italian Chapter Conference, 2014, pp. 41–44.

[20] L. Bonaldi, E. Menti, L. Ballerini, A. Ruggeri, and E. Trucco, "Automatic generation of synthetic retinal fundus images: Vascular network," Procedia Computer Science, vol. 90, pp. 54–60, 2016.

[21] J. M. Bower, H. Cornelis, and D. Beeman, "Genesis, the general neural simulation system," Encyclopedia of Computational Neuroscience, pp. 1287–1293, 2015.

[22] N. T. Carnevale and M. L. Hines, The NEURON book. Cambridge University Press, 2006.

[23] G. A. Ascoli and J. L. Krichmar, "L-neuron: a modeling tool for the efficient generation and parsimonious description of dendritic morphology," Neurocomputing, vol. 32, pp. 1003–1011, 2000.

[24] Thota, N.B.; Reddy, D.U. Improving the Accuracy of Diabetic Retinopathy Severity Classification with Transfer Learning. In Proceedings of the 2020 IEEE 63rd International Midwest Symposium on Circuits and Systems (MWSCAS), Springfield, MA, USA, 9–12 August 2020; pp. 1003–1006.

[25] Wang, X.-N.; Dai, L.; Li, S.-T.; Kong, H.-Y.; Sheng, B.; Wu, Q. Automatic Grading System for Diabetic Retinopathy Diagnosis Using Deep Learning Artificial Intelligence Software. Curr. Eye Res. 2020, 45, 1550–1555.

[26] Gangwar, A.K.; Ravi, V. Diabetic Retinopathy Detection Using Transfer Learning and Deep Learning. In Evolution in Computational Intelligence; Springer: Singapore, 2020; pp. 679–689. Panigrahi, P.K.; Mukhopadhyay, S.; Pratiher, S.; Chhablani, J.; Mukherjee, S.; Barman, R.; Pasupuleti, G. Statistical classifiers on local binary patterns for optical diagnosis of diabetic retinopathy. Nanophotonics 2018, 10685, 106852Y.

[27] Pour, A.M.; Seyedarabi, H.; Jahromi, S.H.A.; Javadzadeh, A. Automatic Detection and Monitoring of Diabetic Retinopathy Using Efficient Convolutional Neural Networks and Contrast Limited Adaptive Histogram Equalization. IEEE Access 2020, 8, 136668–136673.

[28] Ramchandre, S.; Patil, B.; Pharande, S.; Javali, K.; Pande, H. A Deep Learning Approach for Diabetic Retinopathy detection using Transfer Learning. In Proceedings of the 2020 IEEE International Conference for Innovation in Technology (INOCON), Bangluru, India, 6–8 November 2020; pp. 1–5.

[29] Bhardwaj, C.; Jain, S.; Sood, M. Deep Learning–Based Diabetic Retinopathy Severity Grading System Employing Quadrant Ensemble Model. J. Digit. Imaging 2021.

[30] Elloumi, Y.; Ben Mbarek, M.; Boukadida, R.; Akil, M.; Bedoui, M.H. Fast and accurate mobile-aided screening system of moderate diabetic retinopathy. In Proceedings of the Thirteenth International Conference on Machine Vision, Rome, Italy, 2–6 November 2020;
Morgan Kaufmann Publishers Inc.: San Francisco, CA, USA, 2021; Volume 11605, p. 116050U.

[31] Z. Wang, W. Yan, and T. Oates. Time series classification from scratch with deep neural networks: A strong baseline. arXiv preprint arXiv:1611.06455, 2016.

[32] D. Wu, M. Zhang, J.-C. Liu, and W. Bauman. On the adaptive detection of blood vessels in retinal images. IEEE Transactions on Biomedical Engineering, 53(2):341–343, Feb 2006.